Imaging

Thallium-201 Imaging and Estimation of Residual High Grade Astrocytoma

Kathy Stafford-Schuck, James M. Mountz, Paul McKeever*, James Taren*, and William H. Beierwaltes

University of Michigan Medical Center, Department of Internal Medicine, Division of Nuclear Medicine, Department of Pathology, and Department of Neurosurgery*, Ann Arbor, Michigan*

Thallium-201 brain imaging was performed on five patients as a method to differentiate persistent and/or recurrent viable Grades III and IV astrocytoma tissue from necrosis or post-therapy changes. Planar images of the head and heart were obtained in order to calculate the ratio of tumor counts to cardiac counts. The heart was chosen as the internal reference organ, as thallium uptake dynamics are reproducible under ordinary circumstances. The numerical estimation of thallium uptake in the brain tumor, expressed in terms of the tumor/cardiac index, correlated well with the clinical course in all five patients. By visual inspection, the initial computed tomographic (CT) and thallium images suggested that the tumors were approximately the same size. Follow-up thallium images were discordant with follow-up CT images. Computed tomography, in general, appeared to depict image alterations suggesting more extensive regrowth of tumor than the actual clinical status or thallium brain scans demonstrated. Histologic examination best correlated with thallium images. In one patient's course of imaging we were able to detect tumor recurrence, by means of thallium imaging, 4 months prior to its appearance on CT. When performed serially, the tumor/cardiac index may provide an estimate of residual tumor burden, which can help distinguish tumor recurrence from changes secondary to therapy.

High grade astrocytoma represents the most common primary malignant brain tumor in the adult, and is associated with high morbidity and mortality (*1*). Therapies for these tumors consist of surgery, chemotherapy, and a variety of methods of irradiation (*2–4*). During therapy one hopes to destroy tumor, but necrosis and edema occur concurrently (*5*). Clinical signs and symptoms of tumor recurrence cannot be reliably distinguished from post-therapy edema and necrosis (*1*). Transmission computed tomography (CT) as well as more standard radionuclide imaging techniques are unable to reliably distinguish persistent and recurrent tumor from necrosis or edema (*6*). The lack of specificity results from the mechanism of localization in contrast enhanced CT and standard radionuclide imaging, which primarily depends on blood–brain barrier breakdown (*7*). Magnetic resonance imaging (MRI) clearly defines the tumor and surrounding edema, but is unable to distinguish persistent and recurrent tumor from peripheral edema and necrosis (*8*). Positron emission tomography (PET) has recently played a role in identifying recurrent glioblastoma using the metabolic tracer ^{18}F-fluorodeoxyglucose (*9,10*). Although this method appears promising, the high cost of PET scans restricts this diagnostic modality to only a few selected centers around the world. Although thallium-201 (^{201}Tl) scanning has been performed on a variety of tumors (*11–13*), more recently ^{201}Tl imaging has been shown to be better correlated with residual high grade glioma tissues as compared with other radionuclide imaging agents such as technetium-99m (^{99m}Tc)-glucoheptonate, ^{99m}Tc-pertechnetate, and gallium-67 (^{67}Ga) (*14*). In this report, Kaplan et al. suggest that ^{201}Tl has a specific mechanism of localization, whereby acting as a potassium analog, it is taken up by viable tumor cells more readily than normal brain cells (*14*). This proposed mechanism of uptake is supported in other studies that indicate ^{201}Tl uptake is related to cellular growth rates (*15,16*). The localization of ^{201}Tl is therefore unique when compared with other standard radionuclide tracers or iodinated contrast media, since its uptake reflects viable tumor and not simply blood–brain barrier breakdown.

Our goal was to determine whether ^{201}Tl imaging could be used to localize and estimate residual Grade III and Grade IV astrocytoma tissue in patients throughout the course of their disease. We hypothesize that increased ^{201}Tl uptake in a patient who is clinically worse suggests tumor recurrence. Conversely, deterioration of clinical status in the face of unchanged ^{201}Tl uptake suggests increasing edema or necrosis. We also report a new method to quantitate the uptake of ^{201}Tl in the tumor: the tumor to cardiac ratio.

MATERIALS AND METHODS

During a 1-yr period planar ^{201}Tl brain imaging was performed on five patients admitted with presumptive diagnosis

For reprints contact: James M. Mountz, MD, Nuclear Medicine, University of Michigan Medical Center, 1500 East Medical Center Drive, Ann Arbor, MI 48109-0028.

of recurrent high grade astrocytoma. The patients (Table 1) were clinically diagnosed as having high-grade astrocytoma, which was confirmed by tumor biopsy. The patients received ^{201}Tl brain scans as part of their routine follow-up, at approximately the same time that they received their initial CT scan at this institution.

Each patient was injected intravenously with 5 mCi of ^{201}Tl in isotonic sodium chloride. Planar 300,000-count images of the head were performed 5 min after injection. Based on tumor location, the view thought to best demonstrate tumor was taken first. This was followed by a 5-min anterior chest image of the cardiac region. Finally the lateral, anterior, posterior, and vertex views of the head were obtained. The anterior chest view was obtained to determine counts in the cardiac region. These cardiac measurements permitted calculation of a numerical estimate of viable tumor mass that could be used in serial comparisons when tumor recurrence was clinically suspected. Follow-up ^{201}Tl studies were acquired using an identical protocol to reproduce thallium localization dynamics for tumor and heart. Imaging was performed on a gamma camera and stored on a 128 × 128 word matrix. Imaging time was recorded for each view. Operator-defined regions of interest were drawn around the tumor and both ventricles of the heart. After background subtraction and correction for differential counting times of the cardiac and tumor regions, the ratio of counts from the tumor region to the cardiac region was calculated as follows:

$$\text{Corrected tumor counts (T)} = \left[C_t - \frac{A_t}{A_b} \times C_b\right] \times S$$

$$\text{Corrected cardiac counts (C)} = \left[C_c - \frac{A_c}{A_b} \times C_b\right]$$

where C_t and C_c are raw tumor and cardiac counts; A_t and A_c are tumor and cardiac region of interest sizes (in pixels); A_b and C_b are background area and counts for the respective regions.

The imaging time correction factor S is defined as:

$$\frac{\text{cardiac imaging time (5 min)}}{\text{tumor imaging time (min)}}$$

TABLE 1. Computed Tomography and Thallium-201 Correlation

Patient	Sex	Age (yr)	Tumor grade	Tumor location	Tumor size (CT diameter, cm)	Baseline T/C index (%)
1	M	38	III	R Parietal	3.5	5.1
2	M	42	IV	L Temporal	5.0	16.5
3	M	49	IV	L Frontal	4.0	12.5
4	M	29	IV	R Frontal/ Parietal	2.5	0.4
5	M	35	III	L Temporal	3.0	2.8

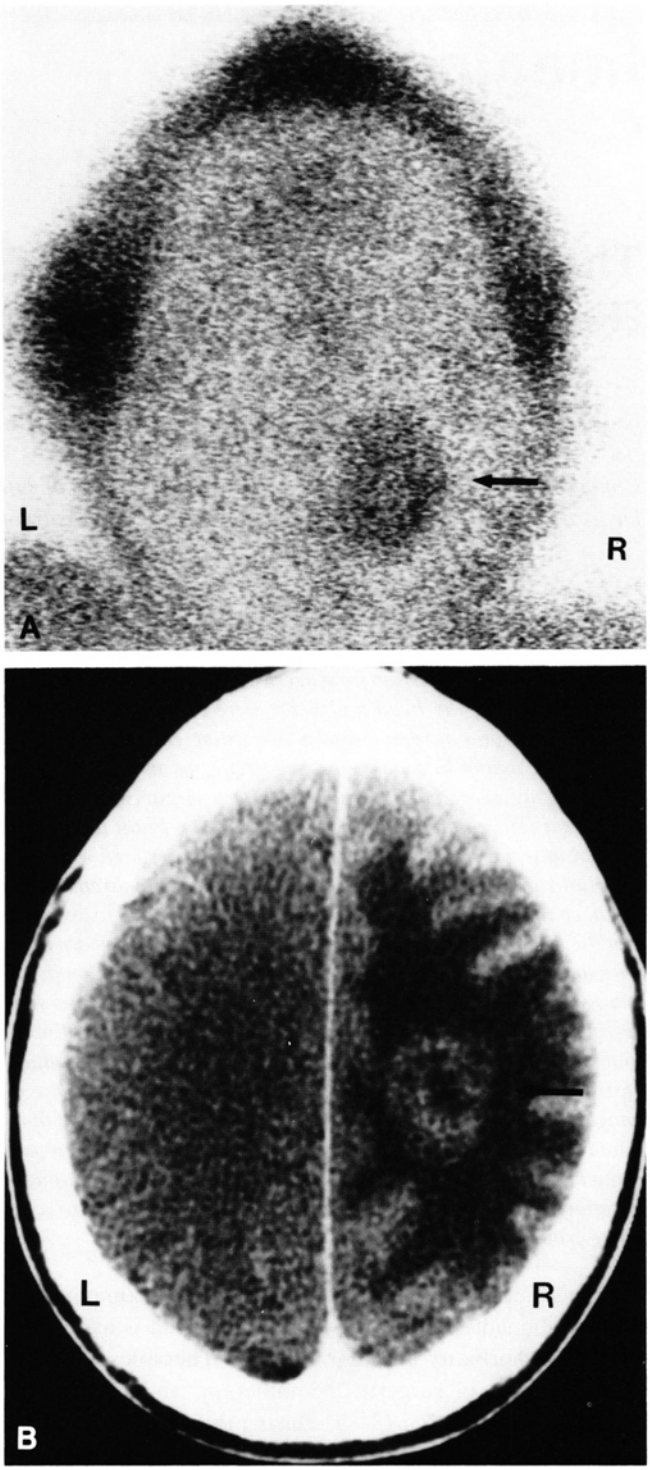

FIG. 1. (A) Baseline planar vertex image showing ^{201}Tl uptake in tumor (arrow). (B) Baseline contrast enhanced CT scan at the level of tumor (arrow).

The tumor to cardiac ratio (T/C) gives a numerical estimate of relative tumor burden. Sequential images in follow-up thallium scans yield T/C indices that are helpful in serial comparison.

RESULTS

The baseline ^{201}Tl brain scans and CT images of all five pa-

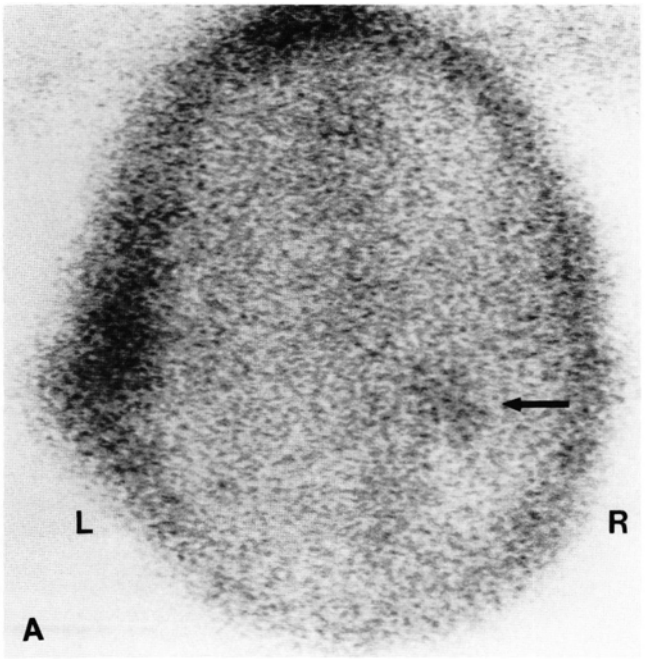

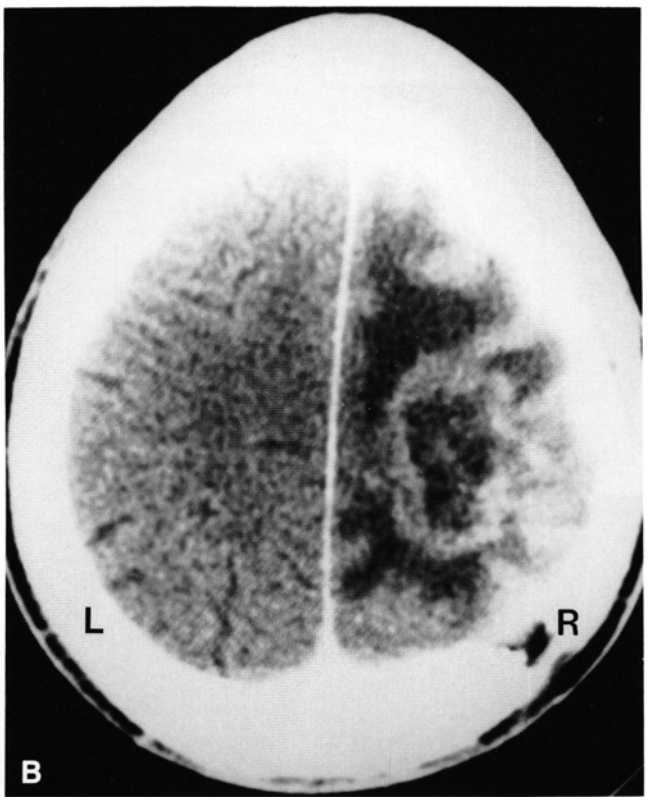

FIG. 2. (A) Post-surgical ^{201}Tl brain scan, vertex image. Note the marked decrease in uptake (arrow) compared with Fig. 1A. (B) Post-surgical contrast enhanced CT scan at the level of tumor. Note the amount of contrast enhancement has not significantly changed compared to the baseline CT scan.

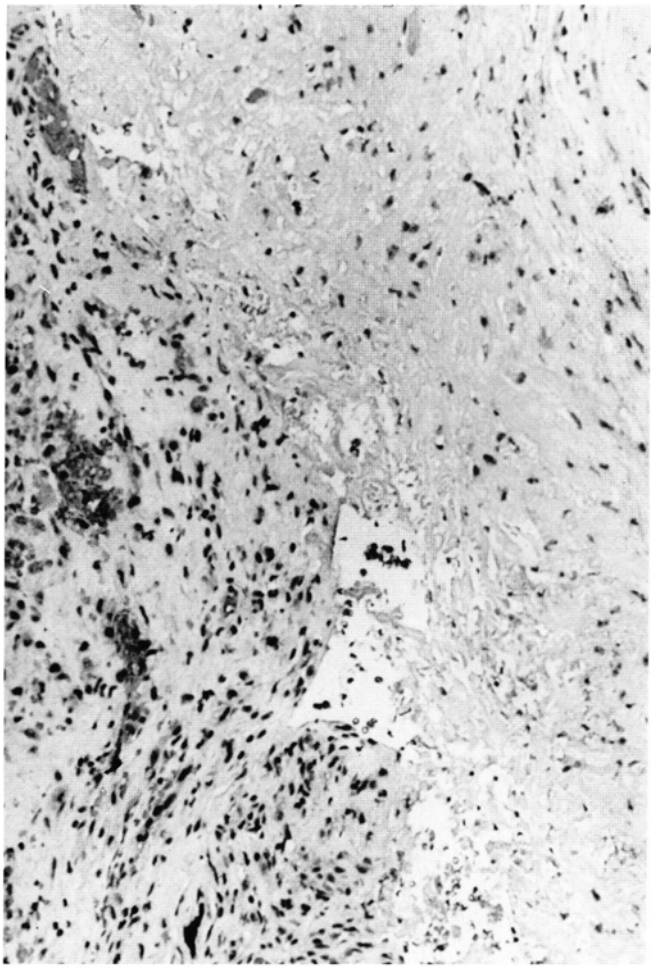

FIG. 3. Surgical specimen demonstrating tumor (left) invading brain (right). Necrotic tissue (not shown) was identified on the histologic section left of tumor.

tients depicted abnormalities in the same location in the brain (Table 1); however, in sequential post-therapy CT and ^{201}Tl scans there was poor correlation, primarily due to the continued presence of edema and contrast enhancement visualized on CT. The ^{201}Tl scans showed marked decrease in tumor uptake immediately after surgery, presumably reflecting the decrease in numbers of viable tumor cells. Sequential imaging was possible in three of five patients.

One patient, a 38-yr-old white male presenting with a Grade III right parietal astrocytoma, was evaluated over a 7-mo period and four serial CT and ^{201}Tl scans were performed. Although the initial CT and ^{201}Tl scans were visually comparable (Fig. 1), after surgical debulking the CT and ^{201}Tl scans became discordant. The CT scan showed little change and demonstrated a contrast enhancing rim, whereas the ^{201}Tl scan demonstrated significantly decreased uptake compared with the pre-surgical scan (Fig. 2). During surgery, core samples extending from central tumor necrosis to normal brain were obtained, and pathologic examination verified a rim of viable high grade astrocytoma tissue around the central area of necrosis (Fig. 3 is the pathology slide for Fig. 1). At pathologic examination most resected tumor margins were free of tumor, and this successful surgical debulking is apparent comparing the pre- and post-surgical ^{201}Tl scans (Fig. 2A compared with Fig. 1A). The T/C index prior to surgery was 5.1% and decreased to

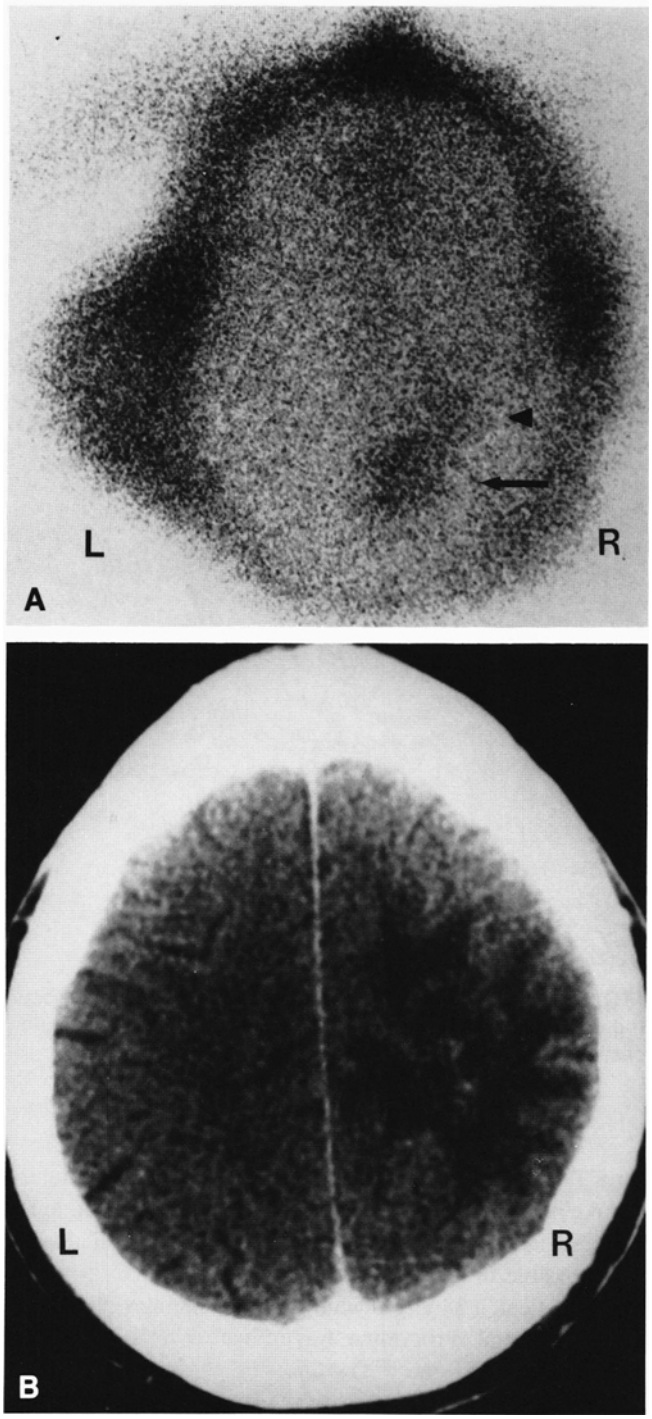

FIG. 4. (A) Four month post-surgery ^{201}Tl scan. Region of increased ^{201}Tl uptake (arrow) is seen posterior and medial to the original tumor site (arrowhead). (B) Four month post-surgery contrast enhanced CT scan fails to show an abnormality in the region of tumor recurrence.

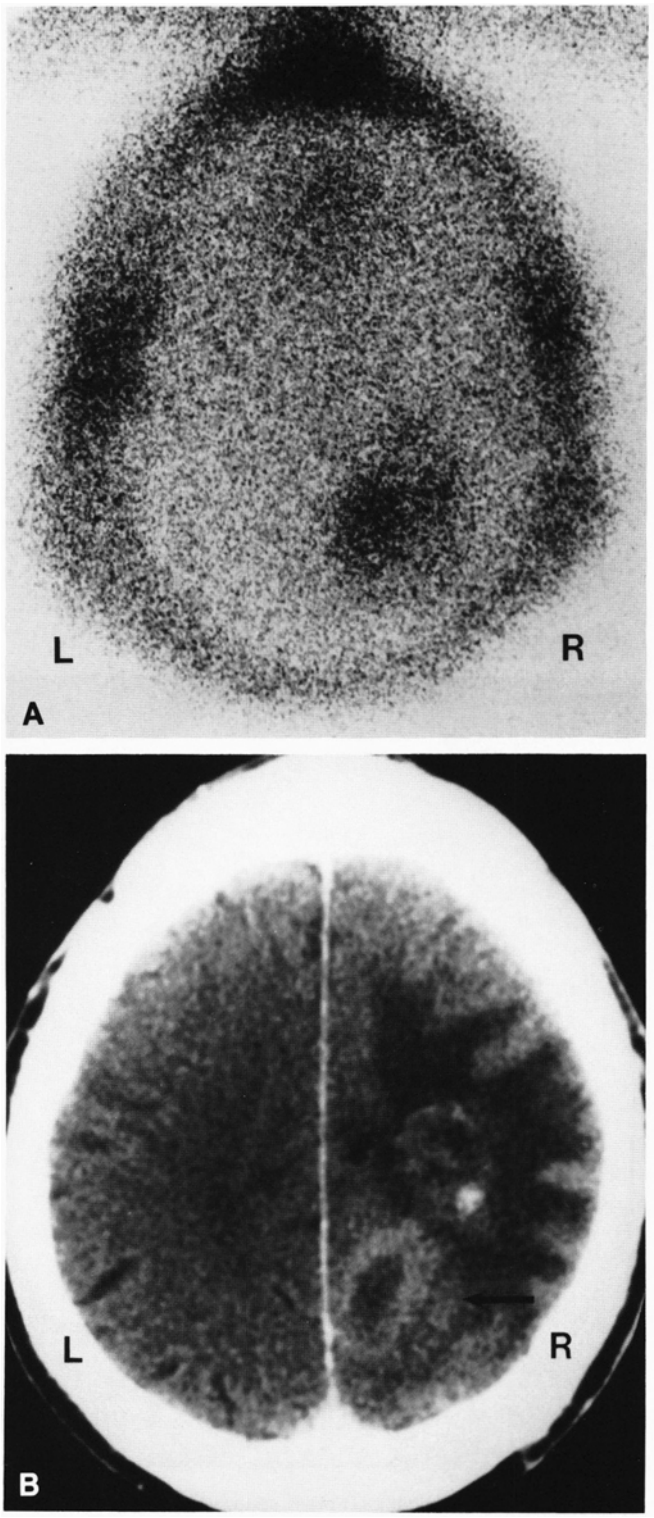

FIG. 5. (A) Six month post-surgery ^{201}Tl scan showing increased uptake in the region of tumor recurrence. (B) Six month post-surgery CT scan demonstrates the site of tumor recurrence (arrow).

0.80% after surgery. This decreased ^{201}Tl uptake after tumor resection is contrasted with the CT scans, which showed little change after resection (Fig. 2B compared with Fig. 1B).

One month after surgery, both CT and ^{201}Tl scans were negative for additional tumor recurrence. At approximately 3 mo after surgery the CT scan remained negative for recurrence and the ^{201}Tl scan T/C index at the original tumor site remained unchanged. There was, however, an area of increased ^{201}Tl uptake (posterior and medial to the original tumor) suggesting new tumor recurrence adjacent to the original primary. The T/C index of this region was determined to be 1.4%. At approximately 6 mo after surgery the CT scan remained nega-

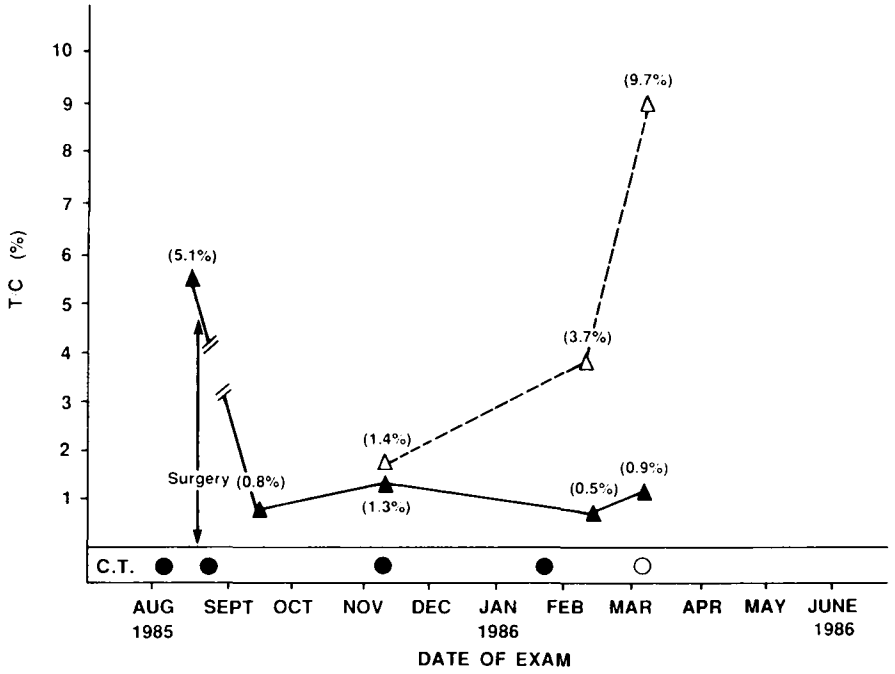

FIG. 6. Chronologic depiction of CT and ^{201}Tl imaging sequence with T/C results: solid line, thallium scan demonstrating uptake in residual tumor only; broken line, thallium scan demonstrating focus of uptake in new tumor recurrence; solid circle, positive CT scan for residual tumor *only*; open circle, positive CT scan for residual tumor and new recurrence; solid triangle, (T/C ratio) primary tumor site; open triangle, (T/C ratio) new tumor recurrence.

tive for recurrence and the ^{201}Tl scan remained essentially unchanged at the original tumor site; however, the new area of ^{201}Tl uptake noted on the prior scan had increased. Although the patient remained asymptomatic at this time, the T/C index for that region increased to 3.7% (Fig. 4A). During the intervening month the patient became symptomatic, developing headaches and lethargy, and the 7-mo follow-up ^{201}Tl scan again demonstrated no change in the original tumor location, but showed increased uptake in the previously described adjacent region (Fig. 5A). The T/C value of the new region increased to 9.7%. The CT scan performed the same day demonstrated an area of pathologic contrast enhancement surrounding an area of low attenuation representing tumor recurrence (Fig. 5B). The recurrence was confirmed by biopsy. The region of tumor recurrence noted on the CT scan was identified on the ^{201}Tl scans performed both 1 and 4 mo earlier. Even in retrospect, analysis of the contrast enhanced CT scans from 1 and 4 mo before failed to reveal an abnormality in the region of new tumor recurrence. Figure 6 graphically illustrates the T/C values and the time course of CT and ^{201}Tl scanning in this patient.

DISCUSSION

Worsening clinical symptoms in a patient with high grade astrocytoma result from either radiation therapy or tumor recurrence. Computed tomography and MRI findings in these cases are usually nonspecific. Thallium-201 is suggested to have specific uptake into tumor cells due to an increase in sodium potassium Na^+/K^+ ATPase activity on tumor cell membranes. Thallium-201 uptake differs from other standard imaging agents, which depend primarily on blood-brain barrier breakdown. We have demonstrated the usefulness of the T/C index as a numerical estimate of residual tumor burden. During the course of imaging in one patient we demonstrated the detection of tumor recurrence 4 mo prior to its appearance on contrast enhanced CT.

CONCLUSION

Thallium-201 imaging of high grade astrocytoma is useful in estimating interval tumor growth. We have demonstrated excellent correlation between clinical findings, pathologic findings, and ^{201}Tl brain scans in patients presenting with residual viable high grade astrocytoma. Planar ^{201}Tl scans allow an estimation of residual or recurrent viable tumor (expressed as T/C) as a numerical index of residual tumor burden. Sequential determinations yield comparative data to determine interval tumor growth throughout the course of the patient's disease.

ACKNOWLEDGMENT

We acknowledge advice and comments suggested by W.D. Kaplan, MD. We also appreciate the excellent secretarial assistance of Mrs. Michele Bell.

REFERENCES

1. Adams RD, Victor M. Intracranial neoplasms. In: Laufer RS, Armstrong T, eds. Principles of Neurology. New York: McGraw-Hill, 1981:440–474.

2. Taasan V, Shapiro B, Taren JA, et al. Phosphorus-32 therapy of cystic Grade IV astrocytomas: Technique and preliminary application. *J Nucl Med* 1985;26:1335–1338.

3. Beierwaltes WH. Horizons in radionuclide therapy: 1985 update. *J Nucl Med* 1985;26:421–427.

4. Leibel SA, Sheline GE, Wara WM, et al. The role of radiation therapy in the treatment of astrocytomas. *Cancer* 1975;35:1551–1557.

5. Marks JE, Gado M. Serial computed tomography of primary brain tumors following surgery, irradiation and chemotherapy. *Radiology* 1977;125:119–125.

6. Moreno JB, DeLand FH. Brain scanning in the diagnosis of astrocytomas of the brain. *J Nucl Med* 1971;12:107–111.

7. Freeman LM, Johnson PM. The central nervous system. In: Freeman LM, ed. Clinical Radionuclide Imaging. 3rd ed. Orlando, FL: Grune and Stratton, 1984:611-723.

8. Brant-Zawadzki M, Badami JP, Mills CM, et al. Primary intracranial tumor imaging: A comparison of magnetic resonance and CT. *Radiology* 1984;150:435-440.

9. Di Chiro G, DeLaPaz RL, Brooks RA, et al. Glucose utilization of cerebral gliomas measured by [^{18}F] fluorodeoxyglucose and positron emission tomography. *Neurology* 1982;32:1323-1329.

10. Patronas NJ, Di Chiro G, Kufta C, et al. Prediction of survival in glioma patients by means of positron emission tomography. *J Neurosurg* 1985;62:816-822.

11. Ancri D, Basset J-Y, Lonchampt MF, et al. Diagnosis of cerebral lesions by thallium-201. *Radiology* 1978;128:417-422.

12. Hisada K, Tonami N, Miyamae T, et al. Clinical evaluation of tumor imaging with ^{201}Tl chloride. *Radiology* 1978;129:497-500.

13. Ancri D, Basset J-Y. Diagnosis of cerebral metastases by thallium-201. *Br J Radiol* 1980;53:443-453.

14. Kaplan WD, Takvorian RW, Morris JH, et al. Thallium-201 brain imaging: A comparative study with pathologic correlation. *J Nucl Med* 1987;28:47-52.

15. Elligsen JD, Thompson JE, Frey HE, et al. Correlation of (Na^+-K^+)-ATPase activity with growth of normal and transformed cells. *Exp Cell Res* 1974;87:233-240.

16. Kasärov LB, Friedman H. Enhanced Na^+-K^+ activated adenosine triphosphatase activity in transformed fibroblasts. *Cancer Res* 1974;34:1862-1865.